PHYSICAL REVIEW B VOLUME 36, NUMBER 17 15 DECEMBER 1987-I

Polaron in n dimensions

Bo E. Sernelius*
Solid State Division, Oak Ridge National Laboratory, Oak Ridge, Tennessee 37831
and Department of Physics, University of Tennessee, Knoxville, Tennessee 37996
(Received 26 May 1987)

The energy dispersion for arbitrary momentum of a polaron in n dimensions is calculated by the Rayleigh-Schrödinger perturbation theory and by a modified Brillouin-Wigner perturbation theory. For the energy and effective mass of the polaron ground state, both methods give results that agree with the results of V. V. Paranjape and P. V. Panjat [Phys. Rev. B **35**, 2942 (1987)] to linear order in the polaron coupling constant α. The self-energy shifts are progressively weakened with increasing dimension. In particular, this weakening occurs for the structure in the energy dispersion near the momentum value at which the polaron starts decaying via the emission of phonons.

I. INTRODUCTION

The polaron problem has been studied actively for several decades. Feynman derived, in an early paper,[1] the ground-state energy and effective mass of the polaron for arbitrary strength of the polar coupling. He used a path-integral method and developed a variational technique in which a trial function for the action was utilized. The fact that the ground-state energy was obtained with a variational technique means that it gave an upper bound for the exact result and all methods giving significantly higher energies can be rejected. Even today there is no theory that works better over the whole range of coupling constants. However, perturbation theory can be used separately in the weak- and strong-coupling limits and can in principle be pushed to arbitrary accuracy. In the weak-coupling expansion (expansion in the coupling constant α) for the ground-state energy and effective mass the expansion coefficients decrease very quickly. The term linear in α actually gives a good approximation to the exact result even in the intermediate coupling regime, i.e., for α up to about three.

In theories of the transport and optical properties of polarons, it is necessary to know the complete dispersion relation and not just the ground-state energy and effective mass. Unfortunately, the perturbation expansion does not work well for all states. In a region of states near where the electron energy is greater than that of the band bottom by an amount equal to the phonon energy, the energy denominators become small or vanish, thus creating a problem. This problem is similar to one in band theory. There, perturbation theory works well away from the band-gap regions, but in those regions it breaks down, again due to small or vanishing energy denominators, and degenerate perturbation theory must be used.

Second-order perturbation theory (producing shifts linear in α) gives an energy that is a nonmonotonic function of momentum. There is a dip in the energy dispersion at p_c, the momentum at which the energy (the unperturbed energy) equals the phonon energy. At this momentum the dispersion has a negative and diverging derivative from the left. The dispersion itself, however, is finite and continuous. Because of the diverging derivative the dip and the nonmonotonicity prevail for all values of α, however small, but the size of this unphysical region around p_c decreases with decreasing α.

Three requirements should be fulfilled for an acceptable theory, viz., the ground-state energy should be given with good accuracy, the structure caused by the resonant coupling to states with one phonon present should occur at a value displaced above the bottom of the shifted band by an amount equal to the phonon energy, and the slope of the dispersion should be nonnegative (or perhaps vanish) at this point. It has been argued[2-4] that the correct behavior for the dispersion in the troublesome region is to have a bend-over and a vanishing derivative at the most critical point.

The Brillouin-Wigner (BW) perturbation theory, known as the Tamm-Dancoff (TD) theory when applied to the polaron problem, can be viewed as a degenerate perturbation theory and gives a more accurate result in the region where the nondegenerate perturbation theory fails. However, it gives very poor results for the ground-state energy. Besides, the structure in the dispersion occurs at a value displaced by an amount equal to the phonon energy above the *unshifted* band bottom, and not above the shifted one, as it should. The improved TD (ITD) theory of Whitfield and Puff[4] eliminates the second problem, but still gives a poor result for the ground-state energy. Larsen[5] developed a variational method based on a combination of the theory of Lee, Low, and Pines[6] (LLP) and the TD theory, which fulfilled all three requirements.

Inspired by the recent interest in lower-dimensional system, Peeters *et al.*[7] derived the result for the polaron ground-state energy in n dimensions using fourth-order perturbation theory within a path-integral formulation. It was found that the perturbation expansion converged faster with increasing dimension. Very recently Paranjape and Panat[8] rederived the result to linear order in α, using an alternative method, the so-called dispersion method. They furthermore calculated the polaron effective mass. It was found that the size of the polaron

 ©1987 The American Physical Society

effects on both the ground-state energy and the effective mass decreased with increasing dimension.

We here rederive the results in Ref. 8 by an alternative method, which we believe to be more familiar to most readers. The result is obtained from the expansion for the exchange and correlation energy for the electron gas in the presence of the coupling to optical phonons by taking the extreme low-density limit in which just one electron is present. The result can also be regarded as the extreme low-density limit of the quasiparticle energy in Rayleigh-Schrödinger (RS) perturbation theory. In this limit both energies coincide. This derivation is presented in Sec. II. The results obtained are linear in α and are identical to those obtained in Ref. 8.

As the polaron effects are weakened with increasing dimension it might be possible to use perturbation theory to obtain accurate results for the energy dispersion at arbitrary momentum. In particular, by studying the energy dispersion at higher dimensions one may hope to get more feeling for how the three-dimensional (3D) dispersion should behave for excitation energies near the phonon energy. The prediction of a vanishing slope, discussed above, is arguable. In our opinion, one can predict only a bend-over and that the derivative should be non-negative.

The question of whether the slope vanishes or not is of physical interest. In a recent paper[9] Hellman and Harris gave a plausible explanation to the puzzling periodic structures observed[10] in the I-V characteristic of GaAs-$Al_xGa_{1-x}As$ tunnel junctions. They suggested that the periodic structures are caused by the vanishing slope in the polaron energy dispersion. The electrons tunnel through the junction and are initially accelerated, but because of the bend-over in the energy dispersion they are subsequently decelerated. A macroscopic number of electrons are collected at a certain distance from the junction. As they each have an energy close to the phonon energy, they will eventually, one by one, drop to the bottom of the band via the emission of a phonon. The acceleration-deceleration process starts over again and the result is that the electrons are bunched in space in a periodic way. This bunching causes the periodic structures in the I-V characteristic. In these experiments the polarons are quasi-one-dimensional but similar effects could appear for 3D polarons if the energy dispersion had a vanishing slope.

We calculate the energy dispersion for arbitrary momentum and find that the size of the polaron effects is reduced with increasing dimension for all momenta. Also, the structure near p_c is weakened. In two dimensions both the energy and its derivative diverge at p_c; in three dimensions only the derivative diverges, while for higher dimensions neither the energy nor the derivative does so. As a complement to this derivation we also use a modified Brillouin-Wigner (MBW) approach which fulfills the three requirements for the 3D case stated earlier. It can be regarded as a simplified version of Larsen's method, but it is not a variational method. This approach is described in Sec. III, where, in addition, the numerical results for the energy dispersion obtained from the two methods are compared. In the 2D case the result from MBW gives three solutions for momentum larger than a certain α-dependent value. In this region a more detailed investigation is needed and we examine the spectral function and its maxima. Finally in Sec. IV we give a brief summary and draw some conclusions.

II. THE ENERGY DISPERSION TO ORDER α FOR A POLARON IN n DIMENSIONS

We define the n-dimensional polaron in the same was as was done in Refs. 7 and 8. The basic interaction is assumed to be the ordinary 3D Coulomb interaction e^2/r, but the electrons are restricted to move in an n-dimensional space. The realizable cases have, of course, $n \leq 3$. For $n < 3$, in our treatment, the electrons move in an n-dimensional space inside the 3D polar semiconductor and the coupling is to the bulk phonons. To take an example, in the 2D case our treatment corresponds to polarons at an interface well inside the bulk of the semiconductor. This is different from the situations treated in the early works on surface polarons by Sak[11] and Evans and Mills.[12] There the polarons were trapped on the surface of a semi-infinite ionic insulator or polar semiconductor and the coupling to surface phonons also entered the problem.

We derive the self-energy shift for the polaron from the expression for the interaction energy $E_{\rm int}$ in a system of electrons and optical phonons.[13] In the absence of phonons this energy is just the exchange and correlation energy. In the presence of phonons it is slightly modified, and can be expressed as

$$E_{\rm int} = -\int_0^1 \frac{d\lambda}{\lambda} \sum_{\mathbf{q}}{}' \int_0^\infty d\omega \frac{\hbar}{2\pi i} \{ [\epsilon_\lambda^{-1}(\mathbf{q},\omega) - 1] - [\epsilon_{0,\lambda}^{-1}(\mathbf{q},\omega) - 1] \} \ . \tag{2.1}$$

As it stands, Eq. (2.1) is valid for n dimensions if the summation over $\mathbf{q}$ is performed in the n-dimensional space. In the expression, which is taken from Eq. (2.25) in Ref. 13, the last term in the integrand comes from the subtraction of the energy contribution from the interaction of each electron with itself. The dielectric function ϵ_0 was introduced to make the physics clearer and to give faster-converging integrals.

The dielectric function for the electrons, $\epsilon_\lambda(\mathbf{q},\omega)$, is given by

$$\epsilon_\lambda(\mathbf{q},\omega) = 1 - \frac{\lambda v_n(\mathbf{q})}{\epsilon_L(\omega)} \chi^0(\mathbf{q},\omega) \ , \tag{2.2}$$

where λ, $v_n(\mathbf{q})$, $\chi^0(\mathbf{q},\omega)$, and $\epsilon_L(\omega)$ are the coupling constant, the Fourier transform of e^2/r in n dimensions, the electron polarizability, and the lattice dielectric function, respectively.

The lattice dielectric function can be expressed as

$$\epsilon_L^{-1}(\omega)=\epsilon_\infty^{-1}+\frac{\omega_L}{2}\frac{\epsilon_0-\epsilon_\infty}{\epsilon_0\epsilon_\infty}\left[\frac{1}{\omega-\omega_L+i\eta}-\frac{1}{\omega+\omega_L-i\eta}\right], \tag{2.3}$$

where ω_L is the frequency of the longitudinal-optical phonon. The constants ϵ_0 and ϵ_∞ are the static and high-frequency dielectric constants, respectively.

The dielectric function $\epsilon^{-1}_{0,\lambda}(\mathbf{q},\omega)$ is defined as

$$[\epsilon^{-1}_{0,\lambda}(\mathbf{q},\omega)-1]=\frac{\lambda v_n(\mathbf{q})}{\epsilon_\infty\hbar\Omega}\sum_{\mathbf{k},\sigma} n_{\mathbf{k},\sigma}\left[\frac{1}{\omega-\omega(\mathbf{k},\mathbf{q})+i\eta}-\frac{1}{\omega+\omega(\mathbf{k},\mathbf{q})-i\eta}\right], \tag{2.4}$$

where Ω denotes the volume of the n-dimensional system, $n_{\mathbf{k},\sigma}$ the occupation number for state $(\mathbf{k},\sigma)$, and

$$\omega(\mathbf{k},\mathbf{q})=(e_{\mathbf{k}+\mathbf{q}}-e_{\mathbf{k}})/\hbar=\frac{\hbar}{2m}[(\mathbf{k}+\mathbf{q})^2-(\mathbf{k})^2], \tag{2.5}$$

i.e., $\hbar\omega(\mathbf{k},\mathbf{q})$ is the change in kinetic energy for an electron in going from state $\mathbf{k}$ to state $\mathbf{k}+\mathbf{q}$.

The extreme low-density limit of Eq. (2.1), taken in such a way that only a single electron in state $\mathbf{p}$ is left in the system, is

$$\Sigma_n(p)=E_{\text{int}}=-\int_0^1\frac{d\lambda}{\lambda}\sum_{\mathbf{q}}{}'\int_{-\infty}^{\infty}d\omega\frac{\hbar}{4\pi i}\left[\frac{\lambda v_n(\mathbf{q})}{\epsilon_L(\omega)\hbar\Omega}\left[\frac{1}{\omega-\omega(\mathbf{p},\mathbf{q})+i\eta}-\frac{1}{\omega+\omega(\mathbf{p},\mathbf{q})-i\eta}\right]-\frac{\lambda v_n(\mathbf{q})}{\epsilon_\infty\hbar\Omega}\left[\frac{1}{\omega-\omega(\mathbf{p},\mathbf{q})+i\eta}-\frac{1}{\omega+\omega(\mathbf{p},\mathbf{q})-i\eta}\right]\right], \tag{2.6}$$

and after integration over the coupling constant it reduces to

$$\Sigma_n(p)=E_{\text{int}}=-\frac{1}{\Omega}\sum_{\mathbf{q}}{}' v_n(\mathbf{q})\int_{-\infty}^{\infty}\frac{d\omega}{2\pi i}[\epsilon_L^{-1}(\omega)-\epsilon_\infty^{-1}]\left[\frac{1}{\omega-\omega(\mathbf{p},\mathbf{q})+i\eta}-\frac{1}{\omega+\omega(\mathbf{p},\mathbf{q})-i\eta}\right]. \tag{2.7}$$

Alternatively, the polaron self-energy can be obtained as the low-density limit of the electron self-energy in the coupled electron-phonon system. Before the limit is taken this energy can be expressed as

$$\Sigma_n(p)=\frac{\delta E_{\text{int}}}{\delta n_{\mathbf{p}}}=-\int_0^1\frac{d\lambda}{\lambda}\sum_{q}{}'\int_{-\infty}^{\infty}\frac{d\omega}{4\pi i}\left[\frac{\lambda v_n(\mathbf{q})}{\epsilon_L(\omega)\epsilon_\lambda^2(\mathbf{q},\omega)\Omega}[G_0(\mathbf{p}+\mathbf{q},e_{\mathbf{p}}/\hbar+\omega)+G_0(\mathbf{p}-\mathbf{q},e_{\mathbf{p}}/\hbar-\omega)]-\frac{\lambda v_n(\mathbf{q})}{\epsilon_\infty\Omega}\left[\frac{1}{\omega-\omega(\mathbf{k},\mathbf{q})+i\eta}-\frac{1}{\omega+\omega(\mathbf{k},\mathbf{q})-i\eta}\right]\right]. \tag{2.8}$$

Integration over the coupling constant gives

$$\Sigma_n(p)=-\frac{1}{\Omega}\sum_{\mathbf{q}}{}' v_n(\mathbf{q})\int_{-\infty}^{\infty}\frac{d\omega}{4\pi i}\left[\frac{G_0(\mathbf{p}+\mathbf{q},e_{\mathbf{p}}/\hbar+\omega)+G_0(\mathbf{p}+\mathbf{q},e_{\mathbf{p}}/\hbar-\omega)}{\epsilon_L(\omega)\epsilon(\mathbf{q},\omega)}-\frac{1}{\epsilon_\infty}\left[\frac{1}{\omega-\omega(\mathbf{p},\mathbf{q})+i\eta}-\frac{1}{\omega+\omega(\mathbf{p},\mathbf{q})-i\eta}\right]\right]. \tag{2.9}$$

We have also changed $\mathbf{q}$ to $-\mathbf{q}$ in the last Green's function. This is allowed because the factor multiplying the Green's function is symmetric with respect to this interchange.

The expression in Eq. (2.9) is useful as it stands for the polaron problem in case there actually are a macroscopic number of electrons present in the band. We are here interested in the energy shifts when only one electron, the electron in state $\mathbf{p}$, is present in the system and therefore we need the extreme low-density limit of the expression. In taking this limit, the dielectric function $\epsilon(\mathbf{q},\omega)$ in the first term becomes unity and the sum of the two Green's functions is reduced to the same expression as that within the set of large parentheses. Thus Eq. (2.7) is obtained again.

Equation (2.7) can be rewritten as

$$\Sigma_n(p)=-\frac{\omega_L}{2}\frac{\epsilon_0-\epsilon_\infty}{\epsilon_0\epsilon_\infty}\frac{1}{\Omega}\sum_{\mathbf{q}}{}' v_n(\mathbf{q})\int_{-\infty}^{\infty}\frac{d\omega}{4\pi i}\left[\frac{1}{\omega-\omega_L+i\eta}-\frac{1}{\omega+\omega_L-i\eta}\right]\times\left[\frac{1}{\omega-\omega(\mathbf{p},\mathbf{q})+i\eta}-\frac{1}{\omega+\omega(\mathbf{p},\mathbf{q})-i\eta}\right]. \tag{2.10}$$

The frequency integrand contains four terms, of which two have their poles on the same side of the real axis. For these terms the contour in the complex ω plane can be closed in the opposite half plane and the corresponding contributions vanish. We are left with the integral

$$\int_{-\infty}^{\infty}\frac{d\omega}{4\pi i}\left[\frac{-1}{(\omega-\omega_L+i\eta)[\omega+\omega(\mathbf{p},\mathbf{q})-i\eta]}+\frac{-1}{(\omega+\omega_L-i\eta)[\omega-\omega(\mathbf{p},\mathbf{q})+i\eta]}\right], \tag{2.11}$$

which we close in the upper half plane and arrive at

$$\frac{1}{\omega(\mathbf{p},\mathbf{q})+\omega_L-i\eta}. \tag{2.12}$$

The expression for the polaron self-energy shift is thus reduced to

$$\Sigma_n(p)=-\frac{\omega_L}{2}\frac{\epsilon_0-\epsilon_\infty}{\epsilon_0\epsilon_\infty}\frac{1}{\Omega}\sum_{\mathbf{q}}{}'v_n(\mathbf{q})\frac{1}{\omega(\mathbf{p},\mathbf{q})+\omega_L-i\eta}. \tag{2.13}$$

The next step towards producing numerical results is to transform the summation over $\mathbf{q}$ into an integral. The result is

$$\Sigma_n(p)=-\frac{\omega_L}{2}\frac{\epsilon_0-\epsilon_\infty}{\epsilon_0\epsilon_\infty}\int_0^\infty\frac{dq}{(2\pi)^n}q^{n-1}v_n(q)\times\int d\Omega_n\frac{1}{\omega(\mathbf{p},\mathbf{q})+\omega_L-i\eta}, \tag{2.14}$$

where the solid angle is given by

$$d\Omega_n=\sin^{n-2}(\theta_{n-1})d\theta_{n-1}\sin^{n-3}(\theta_{n-2})d\theta_{n-2}\cdots d\theta_1. \tag{2.15}$$

As the only angular dependence in the integrand involves the angle between $\mathbf{q}$ and $\mathbf{p}$, we choose this angle to be the angle with highest index. The lowest-index angle is restricted to values between 0 and 2π, while the rest of the angles vary between 0 and π. This expression was also used in Ref. 8. We integrate out all higher-index angles, which yields the result

$$\int d\Omega_n=\int_{-1}^{1}dx\frac{2(1-x^2)^{(n-3)/2}\pi^{(n-1)/2}}{\Gamma\left[\frac{n-1}{2}\right]}, \tag{2.16}$$

where the variable x is the cosine of the angle between $\mathbf{p}$ and $\mathbf{q}$.

The Fourier transform of e^2/r becomes, in n dimensions,

$$v_n(\mathbf{q})=\int_0^\infty dr\,r^{n-1}\int d\Omega_n\frac{e^2}{r}=\frac{\Gamma\left[\frac{n-1}{2}\right](2\pi)^n e^2}{2\pi^{(n+1)/2}q^{n-1}}. \tag{2.17}$$

Inserting Eqs. (2.16) and (2.17) into Eq. (2.14) gives

$$\Sigma_n(p)=-\frac{\omega_L}{2}\frac{\epsilon_0-\epsilon_\infty}{\epsilon_0\epsilon_\infty}\frac{e^2}{\pi}\times\int_0^\infty dq\int_{-1}^{1}dx\frac{(1-x^2)^{(n-3)/2}}{(e_{\mathbf{p}+\mathbf{q}}-e_{\mathbf{p}})/\hbar+\omega_L-i\eta}. \tag{2.18}$$

Let us now introduce some suitable units. Let all wave numbers be expressed in units of p_c, where p_c is

$$p_c=(2m\omega_L/\hbar)^{1/2}, \tag{2.19}$$

i.e., the wave number at which the unperturbed energy equals the phonon energy. To make the notation clearer we use capital letters to denote transformed wave numbers, i.e., $P=p/p_c$ and $Q=q/p_c$.

This transforms Eq. (2.18) into

$$\Sigma_n(P)=-\alpha\hbar\omega_L\frac{1}{\pi}\int_0^\infty dQ\int_{-1}^{1}dx\frac{(1-x^2)^{(n-3)/2}}{Q^2+2QPx+1-i\eta}, \tag{2.20}$$

where the polaron coupling constant α is defined as

$$\alpha=\frac{e^2p_c}{2\hbar\omega_L}\frac{\epsilon_0-\epsilon_\infty}{\epsilon_0\epsilon_\infty}. \tag{2.21}$$

Integration over Q gives the following final result:

$$\Sigma_n(P)=-\alpha\hbar\omega_L\left[\int_0^{\min(1,1/P)}dx\frac{(1-x^2)^{(n-3)/2}}{[1-(xP)^2]^{1/2}}+i\theta(P-1)\int_{P-(P^2-1)^{1/2}}^{P+(P^2-1)^{1/2}}dQ\frac{1}{Q}\left[1-\frac{(1+Q^2)}{2QP}\right]^{(n-3)/2}\right]. \tag{2.22}$$

Before presenting numerical results for general P let us study some limits. The polaron ground-state energy is given by

$$E_n(0)=-\alpha\hbar\omega_L\int_0^1dx(1-x^2)^{(n-3)/2}=-\alpha\hbar\omega_L\frac{\sqrt{\pi}}{2}\frac{\Gamma\left[\frac{n-1}{2}\right]}{\Gamma\left[\frac{n}{2}\right]}. \tag{2.23}$$

The polaron effective mass is obtained from the derivative of Eq. (2.22) for vanishing wave number according to

$$m_{\rm pol}^{-1}=m^{-1}\left[1+\frac{1}{2\hbar\omega_L}\left[\frac{1}{P}\frac{d\Sigma(P)}{dP}\right]_{P=0}\right]=m^{-1}\left[1-\frac{\alpha}{2}\int_0^1 dx(1-x^2)^{(n-3)/2}x^2\right]$$
$$=m^{-1}\left[1-\alpha\frac{\sqrt{\pi}}{4n}\frac{\Gamma\left[\frac{n-1}{2}\right]}{\Gamma\left[\frac{n}{2}\right]}\right]. \tag{2.24}$$

These results are in agreement with Ref. 8.

It is furthermore found from inspection of Eq. (2.22) that

$$\mathrm{Re}\Sigma_n(1)=\mathrm{Re}\Sigma_{n-1}(0)=-\alpha\hbar\omega_L\frac{\sqrt{\pi}}{2}\frac{\Gamma\left[\frac{n-2}{2}\right]}{\Gamma\left[\frac{n-1}{2}\right]}=(\alpha\hbar\omega_L)^2\frac{\pi}{2(n-2)}\Sigma_n^{-1}(0)\ . \tag{2.25}$$

In 3D the integral in Eq. (2.22) can be performed analytically and the result is

$$\Sigma_3(P)=-\alpha\hbar\omega_L\left[\theta(1-P)\frac{1}{P}\sin^{-1}(P)+\theta(P-1)\left[\frac{\pi}{2P}+\frac{i}{2P}\ln\left|\frac{P+(P^2-1)^{1/2}}{P-(P^2-1)^{1/2}}\right|\right]\right]. \tag{2.26}$$

In 2D the expression for the real part can be identified as complete elliptical integrals of the first kind both for $P<1$ and for $P>1$. The same result as ours for $P<1$ was obtained in Ref. 14. However, in that reference was found, in contradiction to our findings, a vanishing shift for $P>1$. In the 4D case the real part can be identified as an incomplete elliptical integral of the second kind for $P>1$.

The numerical results for the real part of the self-energy shifts are shown in Fig. 1 for various n values. It cannot be obtained for a strictly one-dimensional system since for that case $v_n(q)$ diverges for all q values. In 2D both the shift and its derivative diverge for $p=p_c$, but are finite and nondivergent everywhere else. In 3D the shift is finite and continuous at p_c but its derivative is discontinuous at that point and the derivative from the left diverges. For four and higher dimensions both the shift and its derivative are continuous everywhere and the structure around p_c becomes progressively weaker with increasing dimension. Also to be noted is that the shift no longer has its minimum at p_c, but rather at a higher p value, and that this p value increases with dimension. From Fig. 1 one further finds that, in accordance with Refs. 7 and 8, the energy shift and effective mass for $p=0$ decrease with increasing dimension. The smaller the curvature which the curves have at $p=0$, the smaller are the effective-mass enhancements. We return to these results for the energy dispersion in the next section, where they are compared to the results from a modified Brillouin-Wigner method.

III. ENERGY DISPERSION FOR THE POLARON FROM A MODIFIED BRILLOUIN-WIGNER APPROACH

In the Brillouin-Wigner (BW) perturbation theory the Dyson's equation is solved for the electron Green's function and the result is

$$G_n(p,\omega)=\frac{1}{\omega-[e_{\rm p}+\Sigma_n'(p,\omega)]/\hbar}\ , \tag{3.1}$$

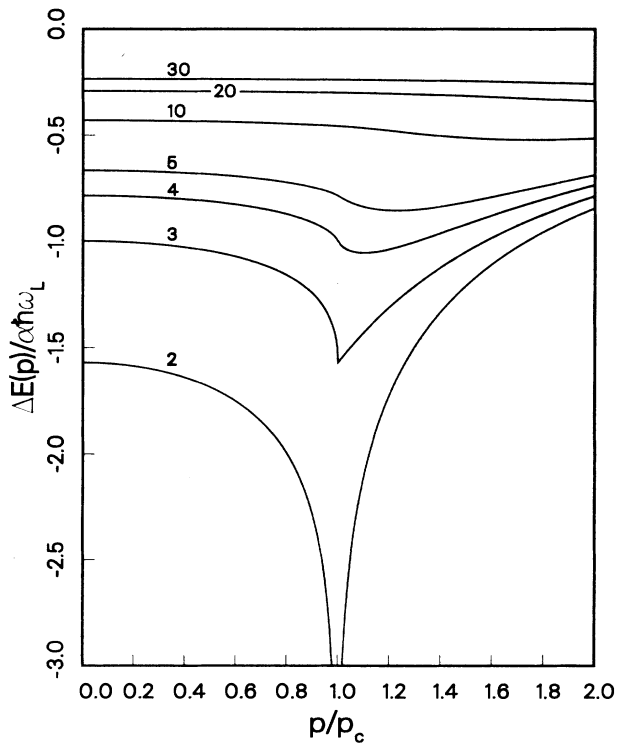

FIG. 1. The interaction-induced energy shifts (the real part) in units of $\alpha\hbar\omega_L$, as a function of wave number, for a series of dimensions. The results are from the Rayleigh-Schrödinger perturbation theory and the numbers labeling the curves are the corresponding dimensions.

where $\Sigma'(q,\omega)$ is the proper self-energy insertion, which we here assume to be to lowest order in the electron-phonon coupling (TD one-quantum cutoff). The energy dispersion is obtained from finding the zeros for the real part of the denominator in Eq. (3.1), i.e.,

$$E_n(p)=e_p+\mathrm{Re}\Sigma'_n(p,E_n(p)/\hbar) \ . \tag{3.2}$$

The self-energy that appears here is different from the one we defined in the previous section. It depends on two variables, wave number and frequency, instead of just the wave number. However, the two self-energies are closely related. The one used here can be obtained by replacing e_p in Eq. (2.18) by $E_n(p)$ or $\hbar\omega$, i.e.,

$$\Sigma_n(p)=\Sigma'_n(p,e_p/\hbar) \ . \tag{3.3}$$

A particularly simple relation can be found between the ground-state energies in BW and in RS. For zero wave number, Eq. (2.20) separates into a product of two integrals, one over Q and one over x. The dimension enters only in the integral over x, while the modification performed in going from RS to BW is in the integral over Q. As a result the energies in the ground state as obtained from RS and BW are related in the same way for all dimensions. In BW the term 1 in the denominator in Eq. (2.20) is replaced by $1+P^2-E_n^{\mathrm{BW}}/\hbar\omega_L$. The integral over Q is straightforward and one finds

$$E_n^{\mathrm{BW}}/\hbar\omega_L=(E_n^{\mathrm{RS}}/\hbar\omega_L)/[1-(E_n^{\mathrm{BW}}/\hbar\omega_L)]^{1/2} \ . \tag{3.4}$$

This is a cubic equation which is easily solved. The same relation has been obtained earlier for the 3D case (see p. 493 of Ref. 15). Thus we find that the $E_n^{\mathrm{BW}}/\hbar\omega_L$ is a universal function of the variable $-E_n^{\mathrm{RS}}/\hbar\omega_L$. This variable is identical to α', introduced in Ref. 7:

$$\alpha'=-E_n^{\mathrm{RS}}/\hbar\omega_L=\frac{\sqrt{\pi}}{2}\frac{\Gamma\left[\frac{n-1}{2}\right]}{\Gamma\left[\frac{n}{2}\right]}\alpha \ . \tag{3.5}$$

The comparison between the BW and RS results is shown in Fig. 2, where we have chosen α' as a variable in order to get a universal curve. For reasons of comparison we also show the results from the Feynman approach[1] (solid curves) and from fourth-order Rayleigh-Schrödinger perturbation theory[7] (dotted curves), for the dimensions 2, 3, and 4. Obviously BW gives much poorer results than RS. This is an example where a summation of an infinite subclass of diagrams gives less-accurate results than those obtained from just keeping a finite number of diagrams. RS gives a result that is only linear in α while BW has contributions to all orders in α and still gives a much poorer result. One also notices in Fig. 2 that RS becomes increasingly more accurate (moves closer to the Feynman result) for increasing dimension.

As we mentioned in the Introduction, BW (or TD) not only produces poor ground-state energies, it also gives the bend-over in the energy dispersion at the wrong position. Whitfield and Puff[4] derived, in a Hartree-Fock–like theory, the so-called improved Tamm-Dancoff (ITD) method. Apart from replacing e_p with $E(p)$ in Eq. (2.18) one also replaces e_{p+q} with $E(\mathbf{p}+\mathbf{q})$ and after certain approximations are introduced one may solve the problem self-consistently. ITD resolved the problem with the position of the bend-over, but still gave very poor ground-state energies. Larsen[5] derived a variational method which resolved both the problems.

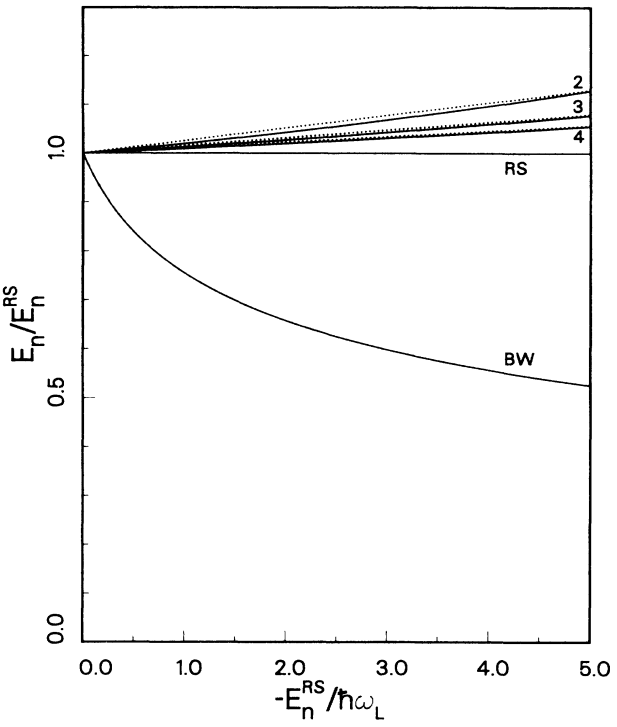

FIG. 2. The polaron ground-state energy for n dimensions, in units of the corresponding result obtained in the Rayleigh-Schrödinger perturbation theory (RS), as a function of the coupling constant, expressed as $-E_n^{\mathrm{RS}}/\hbar\omega_L$. The Brillouin-Wigner result (BW) is valid for all dimensions, which is not the case for the Feynman results (solid curves) and those from the fourth-order Rayleigh-Schrödinger perturbation theory (dotted curves), which are here given for the three dimensions 2, 3, and 4.

We use a modified BW (MBW) method, which can be regarded as a simplified version of Larsen's method. The polaron energy is obtained from

$$E_n(p)=e_p+\mathrm{Re}\Sigma'_n(p,[E_n(p)-E_n(0)]/\hbar) \ , \tag{3.6}$$

which is the same as Eq. (3.2) except that the ground-state energy has here been subtracted in the energy argument. This forces the ground-state energy to become identical to the RS result. Equation (3.6) also produces a bend-over in the energy dispersion at the correct position.

Introduction of the variable

$$y=E_n(p)-e_p-E_n(0) \tag{3.7}$$

reduces Eq. (3.6) to

$$y=\mathrm{Re}\Sigma'_n(p,(e_p+y)/\hbar)-E_n(0) \ . \tag{3.8}$$

It can be further simplified to

$$Y=[\mathrm{Re}\Sigma_n(P/\sqrt{1-Y})/\sqrt{1-Y}-E_n(0)]/\hbar\omega_L\ , \quad (3.9)$$

where $Y=y/\hbar\omega_L$. This expression involves the self-energy in RS, given in Eq. (2.22).

The 3D results for the energy dispersion from MBW (solid curves) are compared in Fig. 3 to those from RS (dotted curves) for the α values 0.25, 0.5, 1, and 2. As a reference the unperturbed dispersion is shown as the dashed curve. One notes the unphysical dip in the RS result at $p=p_c$. The MBW dispersion bends over and has a vanishing slope at the energy $\hbar\omega_L$ above the band bottom. For higher energies MBW and RS give identical results. The dispersion near the bottom of the band is given by the effective mass. m/m^* has the following α expansions in the different approaches:

$$\left.\frac{m}{m_{\rm pol}}\right|_{\rm MBW}=1-\frac{\alpha}{6+3\alpha}=1-\frac{\alpha}{6}+\frac{\alpha^2}{12}-\cdots\ ,$$

$$\left.\frac{m}{m_{\rm pol}}\right|_{\rm Larsen}=1-\frac{\alpha}{6+\alpha/2}=1-\frac{\alpha}{6}+\frac{\alpha^2}{72}-\cdots\ ,$$

$$\left.\frac{m}{m_{\rm pol}}\right|_{\rm RS}=1-\frac{\alpha}{6}\ , \quad (3.10)$$

$$\left.\frac{m}{m_{\rm pol}}\right|_{\rm RS4}=1-\frac{\alpha}{6}+0.022\,63\alpha^2\ ,$$

$$\left.\frac{m}{m_{\rm pol}}\right|_{\rm Feynman}=1-\frac{\alpha}{6}+\frac{\alpha^2}{360}\cdots\ .$$

The fourth-order Rayleigh-Schrödinger (RS4) result was obtained in Ref. 16. As can be seen, all results agree to linear order in α.

The 4D results are shown in Fig. 4 for the same set of α values. The notation is the same as in Fig. 3. The unphysical nonmonotonicity in the dispersion from RS also occurs here, but only for high α values. The MBW dispersion bends over at $\hbar\omega_L$ above the band bottom, as it should, but it should be noted that this bend-over is much weaker here than in the 3D case and the slope does not vanish. This leads one to suspect that maybe the vanishing slope in 3D should not be there. In BW, ITD, Larsen's method and MBW it is there because of the diverging derivative of the RS self-energy at p_c. If one used a higher-order self-energy insertion the vanishing slope might disappear.

Another difference compared to the 3D case is that here the MBW and RS are not identical for energies above $\hbar\omega_L$. Actually, all the curves, solid, dotted, and dashed, have two points in common. One is the band bottom. The second point is for the wave number at which the RS self-energy is the same as at the band bottom. In Fig. 4 this point is outside the plot.

In 2D we found (see Fig. 1) that the RS gave stronger shifts near p_c than in 3D and one would expect the MBW energy dispersion in 2D to show pronounced structures. This is also found. The 2D dispersions are shown in Fig. 5. The dispersions bend over and the energy approaches $\hbar\omega_L$ as $p\to\infty$. For p larger than a cer-

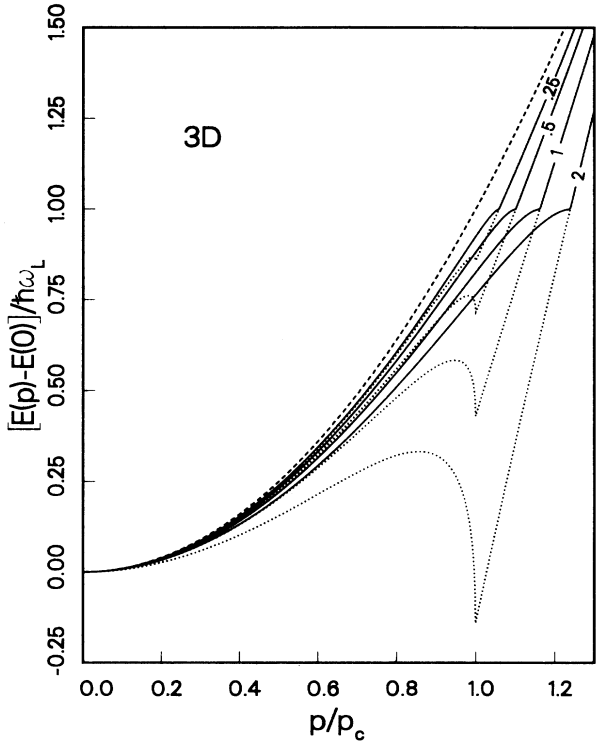

FIG. 3. The polaron energy dispersion in 3D in units of $\hbar\omega_L$ for the coupling constants 0.25, 0.5, 1, and 2. The dotted curves represent the Rayleigh-Schrödinger results and the solid curves the modified Brillouin-Wigner results. The dashed curve is the unperturbed electron dispersion.

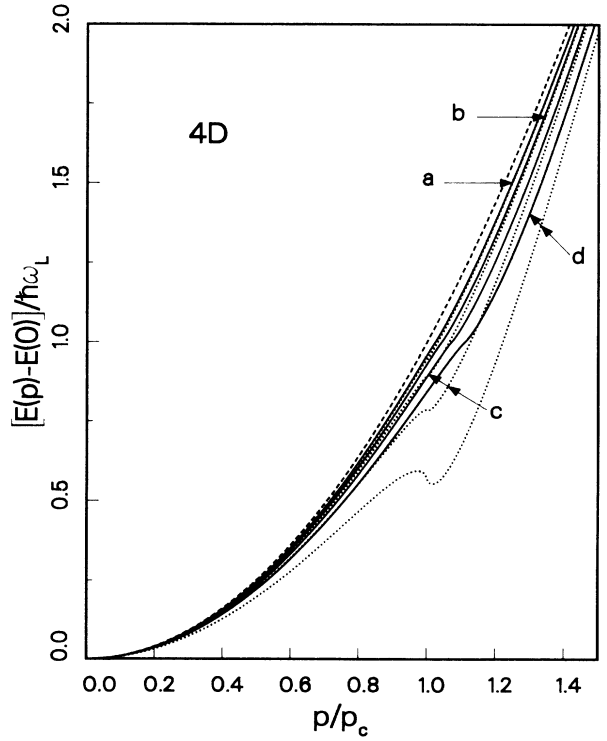

FIG. 4. The same as Fig. 3 but now for 4D. The letters a, b, c, and d denote the coupling constants 0.25, 0.5, 1, and 2, respectively.

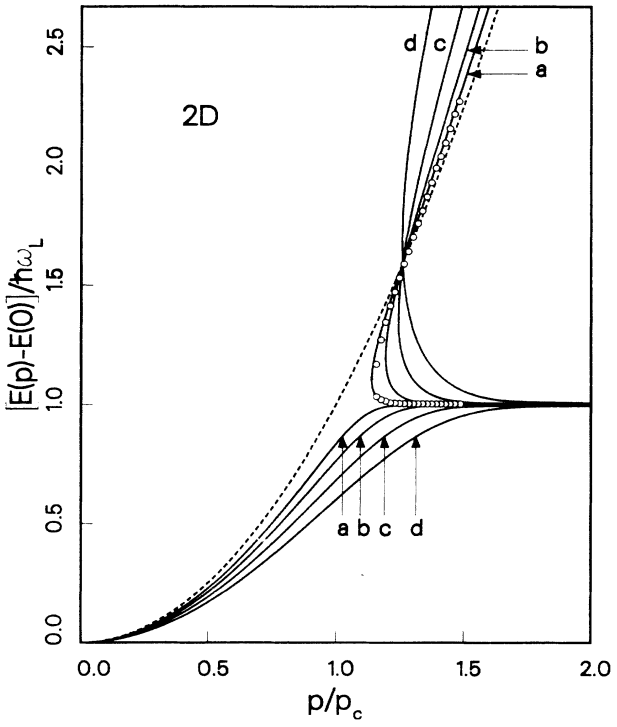

FIG. 5. The same as Fig. 4 but now for 2D. The notation is unchanged. The additional open circles indicate the positions of the peaks in the continuum part of the spectral function for the coupling constant 0.25.

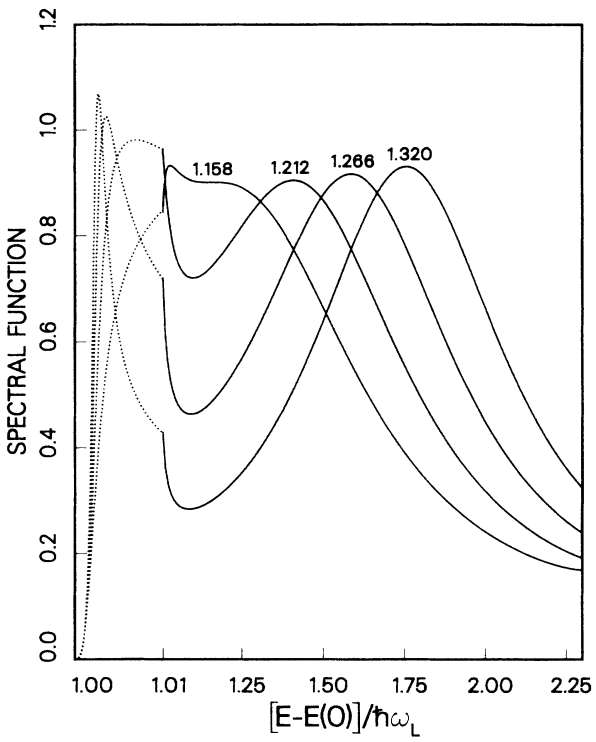

FIG. 6. The continuum part of the spectral function of 2D polarons for four different wave numbers. The wave numbers are indicated above each corresponding curve. The plot is expanded in the energy region between 1.0 and 1.01, and to avoid confusion the curves are dotted in that region.

tain α-dependent value, Eq. (3.6) has three solutions. For energies above $\hbar\omega_L$, however, the imaginary parts of the self-energies are nonzero. This is the case in all dimensions, not only in 2D. It means that the polaron is no longer a stable excitation of the system. It decays via emission of longitudinal-optical phonons. If this decay is weak enough the polaron is still a useful concept. The spectral function gives information about how well defined an excitation is. We have, in Fig. 5, complemented the curve for $\alpha=0.25$ with the peak positions in the corresponding spectral function. We can see that the peak positions, at least for small α values, agree quite well with the solutions to Eq. (3.6). The spectral function consists of a δ function in the branch below $\hbar\omega_L$ and a double-peak structure for energies above $\hbar\omega_L$. The part above $\hbar\omega_L$ is given for a set of p values in Fig. 6. For large p values it consists of two well-resolved peaks. The peak at highest energy corresponds to the excitation one would expect to find. Its dispersion approaches that for an unperturbed electron as $p\rightarrow\infty$. The other peak is very narrow and close to the energy $\hbar\omega_L$. In order to resolve the narrow peaks we have expanded the plot for energies just above $\hbar\omega_L$. The curves are dashed in the expanded part of the plot. With increasing p the narrow peak becomes even narrower which indicates that this excitation becomes more well defined. However, the integrated area under the peak decreases.

IV. SUMMARY AND CONCLUSION

We have studied the energy dispersion for polarons in n dimensions, as obtained from the Rayleigh-Schrödinger perturbation theory and from a modified Brillouin-Wigner perturbation theory. We found that the structure in the dispersion, caused by the resonant coupling to states with one phonon present, decreased with increasing dimension.

It has been argued that the dispersion should have a bend-over and a vanishing slope at the point above the band bottom equal to the phonon energy. The conclusion that the slope actually vanishes, at the point where the resonant coupling to states with a phonon present sets in, has been arrived at by using Brillouin-Wigner perturbation theory or related theories. The results for dimensions higher than three lead us to question this conclusion. For higher dimensions these theories produce a bend-over which is, however, not strong enough to give a vanishing slope. The vanishing slope obtained in 3D is caused by the diverging momentum derivative of the self-energy insertion used. Using a higher-order self-energy insertion may also give a nonvanishing slope in 3D.

In 2D we found, for momentum larger than a certain coupling-constant-dependent value, three excitations with the same momentum. This result was obtained by the modified Brillouin-Wigner method and also verified from the study of the spectral function.

ACKNOWLEDGMENTS

Research support is acknowledged from the University of Tennessee, Oak Ridge National Laboratory, and the U.S. Department of Energy (through the Oak Ridge National Laboratory, operated by Martin Marietta Energy Systems, Inc.), under Contract No. DE-AC05-840R21400. Support from the Swedish Natural Science Research Council is also acknowledged.

---

*Permanent address: Department of Physics and Measurement Technology, University of Linköping, S-581 83 Linköping, Sweden.

[1]R. P. Feynman, Phys. Rev. **97**, 660 (1955).
[2]T. D. Schulz, MIT Technical Report No. 9, 1956 (unpublished).
[3]G. Whitfield and R. D. Puff, Phys. Lett. **10**, 9 (1964).
[4]G. Whitfield and R. Puff, Phys. Rev. **139**, A338 (1965).
[5]D. M. Larsen, Phys. Rev. **144**, 697 (1966).
[6]T. D. Lee, F. E. Low, and D. Pines, Phys. Rev. **90**, 297 (1953).
[7]F. M. Peeters, Wu Xiaoguang, and J. T. Devreese, Phys. Rev. B **33**, 3926 (1986).
[8]V. V. Paranjape and P. V. Panat, Phys. Rev. B **35**, 2942 (1987).
[9]E. S. Hellman and J. S. Harris, Jr., Phys. Rev. B **33**, 8284 (1986).
[10]T. W. Hickmott, P. M. Solomon, F. F. Fang, and F. Stern, Phys. Rev. Lett. **23**, 2053 (1984).
[11]J. Sak, Phys. Rev. B **6**, 3981 (1972).
[12]E. Evans and D. L. Mills, Phys. Rev. B **8** 4004 (1973).
[13]Bo E. Sernelius, Phys. Rev. B **36**, 4878 (1987).
[14]S. Das Sarma, Phys. Rev. B **27**, 2590 (1983).
[15]G. D. Mahan, *Many-Particle Physics* (Plenum, New York, 1981).
[16]P. Sheng and J. D. Dow, Phys. Rev. B **4**, 1343 (1971).